Inorganic Chemistry

Article

pubs.acs.org/IC

$Cs_8[Fe_4S_{10}]$ and $Cs_7[Fe_4S_8]$, Two New Sulfido Ferrates with Different Tetrameric anions

Michael Schwarz and Caroline Röhr*

Institut für Anorganische und Analytische Chemie, Albert-Ludwigs-Universität Freiburg, Freiburg im Breisgau, Germany

Supporting Information

ABSTRACT: The two new cesium sulfido ferrates $Cs_8[Fe_4S_{10}]$ and $Cs_7[Fe_4S_8]$ were synthesized at a maximum temperature of 1070 K in corundum crucibles from stoichiometric samples containing elemental Fe and S together with cesium disulfide, Cs_2S_2. Their crystal structures have been determined by means of single-crystal X-ray diffraction. $Cs_8[Fe^{III}_4S_{10}]$ crystallizes in the triclinic $Cs_6[Ga_4Se_{10}]$-type structure and is thus isotypic to the corresponding rubidium salt. The structure exhibits tetramers $[Fe_4S_{10}]^{8-}$ of edge-sharing tetrahedra, which represent segments of the well-known chain compounds $A[FeS_2]$. The monoclinic mixed-valent iron(II/III) sulfido ferrate $Cs_7[Fe_4S_8]$, which is isotypic to the cesium tellurido ferrate, likewise contains oligomeric tetramers of four edge-sharing $[FeS_4]$ tetrahedra, in this case resulting in only slightly distorted tetrahedral $[Fe_4S_8]^{7-}$ anions with a Fe_4S_4 cubane core resembling the prominent $[Fe_4(\mu_3\text{-}S_4)]^+$ cluster, e.g., in the active site of ferredoxins. These sulfido ferrate anions are surrounded by 26 Cs cations, which are located at the 8 corners, 6 faces, and 12 edges of a cube. A dense stacking of these cubes, which ultimately results in the overall seven cesium countercations per cluster anion, describes the overall crystal structure completely. According to this arrangement of cluster-centered cubes, a relationship of the packing of Cs cations and cluster anions with the simple cubic packing (α-Po-type structure) can be established by applying the crystallographic group−subgroup formalism. FP-LAPW band-structure calculations applying antiferromagnetic spin ordering of the high-spin Fe ions in the two tetramers predict a small band gap of 1 eV associated with a L → M-CT for $Cs_8[Fe^{III}_4S_{10}]$ and a tiny energy gap of 0.1 eV resulting from a d−d transition for the mixed-valent cluster compound $Cs_7[Fe^{II/III}_4S_8]$.

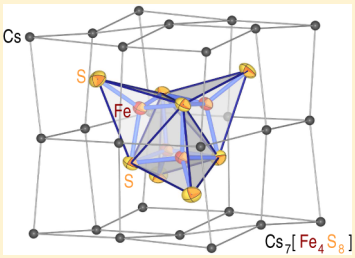

INTRODUCTION

The crystal chemistry of alkali sulfido ferrates $A_x[Fe_yS_z]$ is dominated by edge-sharing $[Fe^{II/III}S_4]$ tetrahedra.[1−4] Depending on the Fe/S ratio, the oxidation state of Fe (which can be II, III, or mixed-valent II/III), and the size of the alkali countercation, the sulfido ferrate anion's connectivity ranges from ortho anions like isolated $[Fe^{II/III}S_4]^{(6/5)-}$ tetrahedra[4−6] (and isolated trigonal-planar anions $[Fe^{II}S_3]^{4-7}$) (Fe:S = 1:4/3), via dimers $[Fe^{III}_2S_6]^{6-}$ of two edge-sharing tetrahedra,[4,8,9] the large series of Fe^{III} and $Fe^{II/III}$ mixed-valent chain ferrates $[FeS_2]^{n-}$ (Fe:S = 1:2),[4,10−15] double chains (in natural/synthetic rasvumites $A[Fe_2S_3]$[16−18] and $Cs_7[FeS_2]_2[Fe_2S_3]_2$[19]) up to layered compounds with the boundary composition $A[Fe_2S_2]$[20−23] and finally three-dimensional nets in the mineral bartonite, $K_7Fe_{21}S_{27}$.[24] Furthermore, solely for the ferrates containing trivalent iron, an infinite series of compounds $A_{n+4}[Fe_nS_{2n+2}]$ may exist between the dimers (Fe:S = 1:3) and the infinite-chain (Fe:S = 1:2) ferrates. The only compound of this hypothetical series known to date is $Rb_8[Fe_4S_{10}]$,[4] which contains linear tetrameric chain pieces $[Fe_4S_{10}]^{8-}$.

In this work, we present the results of a systematic experimental study of phase formation in the corresponding section of the ternary phase diagram Cs−Fe−S, i.e., at Fe:S ratios between 1:2 and 1:2.5. In this composition range, the two new compounds $Cs_8[Fe_4S_{10}]$, which crystallizes isotypic to the above-mentioned rubidium compound, and the mixed-valent ferrate $Cs_7[Fe_4S_8]$ containing likewise tetrameric anions have been successfully prepared in pure phase. Their crystal structures have been determined from single-crystal X-ray data. For $Cs_7[Fe_4S_8]$, the metric features of the cubane-type cluster core are compared to the geometric properties of related iron−sulfur clusters $[Fe_4(\mu_3\text{-}S_4)]^{n+}$ in protein-bound systems and their synthetic analogues. Density functional theory (DFT) band-structure calculations performed by adopting the antiferromagnetic (AFM) spin ordering observed in all known compounds of this type enable a deeper insight into the chemical bonding of both title compounds.

EXPERIMENTAL SECTION

Preparation. The two cesium sulfido ferrates $Cs_8[Fe_4S_{10}]$ and $Cs_7[Fe_4S_8]$ were synthesized in corundum crucibles sealed in steel autoclaves in an argon atmosphere at a maximum temperature of 1070 K. The samples were heated to this temperature at a rate of 50 K/h, held there for 12 h, and subsequently cooled to room temperature at a rate of 20 K/h. The starting materials used were iron filings dried in a drying cabinet, elemental S, and cesium disulfide Cs_2S_2, which was obtained by carefully reacting a solution of elemental Cs (Alkalimetallhandelsgesellschaft Maassen, Bonn, Germany; approximately 3 g) in liquid ammonia with equal amounts of elemental S, following a protocol adapted from the synthesis of the corresponding potassium salts by Brauer.[25] After the preparations, representative

Special Issue: To Honor the Memory of Prof. John D. Corbett

Received: October 1, 2014
Published: December 16, 2014

dx.doi.org/10.1021/ic502382v | Inorg. Chem. 2015, 54, 1038−1048

parts of the reguli were ground and sealed in capillaries with a diameter of 0.3 mm. Powder X-ray diagrams were collected on transmission powder diffraction systems (STADI-P, linear PSD, Fa. Stoe & Cie, Darmstadt, Mo $K\alpha_1$ radiation, graphite monochromator). For phase analysis, the measured powder diagrams were compared to the calculated (program *Lazy-Pulverix*[26]) reflections of the title compounds and other known phases in the system Cs−Fe−S.

In analogy to the isotypic rubidium compound,[4] $Cs_8[Fe_4S_{10}]$ was obtained in pure phase from stoichiometric mixtures of the above-mentioned starting materials, e.g., from a sample containing 492.7 mg (1.49 mmol) of Cs_2S_2, 84.5 mg (1.51 mmol) of Fe, and 24.4 mg (0.76 mmol) of elemental S.

The new cluster compound $Cs_7[Fe_4S_8]$ was obtained for the first time from a sample containing O as a second chalcogen with the overall composition Cs:Fe:S:O = 5:4:6:2 [594.0 mg (1.80 mmol) of Cs_2S_2, 201.0 mg (3.60 mmol) of Fe, 147.7 mg (0.90 mmol) of CsO_2, and 57.1 mg (1.78 mmol) of S]. In this case, the second title compound is accompanied by the mixed-valent chain ferrate $Cs_3[Fe_2S_4]$.[15] Knowing the exact composition, the cesium tetraferrate $Cs_7[Fe_4S_8]$ could be likewise prepared in pure phase from stoichiometric samples composed of, e.g., 655.1 mg (1.99 mmol) of Cs_2S_2, 127.1 mg (2.28 mmol) of Fe, and 19.2 mg (0.60 mmol) of S.

Crystal Structure Determination. For the crystal structure determinations, irregularly shaped single crystals of the two title compounds were selected from the samples using a stereomicroscope. The dark-green metallic shiny crystals were fixed in glass capillaries (diameter 0.1 mm) under dried paraffin oil and centered on a diffractometer equipped with a microsource and a CCD area detector.

The diffraction data of $Cs_8[Fe_4S_{10}]$ showed only triclinic symmetry with lattice constants slightly larger than those for the isotypic rubidium phase.[4] Using the atomic parameters of this structure model as the starting values, the intensity data of $Cs_8[Fe_4S_{10}]$ directly refine (program *SHELXL-2013*[29]) to a conclusively low R value of 0.0410.

The crystals of $Cs_7[Fe_4S_8]$ exhibit a monoclinic C-centered lattice. The systematic absence condition "reflections $h0l$ only present for l = 2 n" ruled out $C2/c$ and Cc as possible space groups. These possible space groups and the dimensions of the lattice parameters suggested isotypism with the corresponding cesium tellurido ferrate[28,30] (and thus also with the selenido cobaltate $Cs_7[Co_4Se_8]$[31]). Starting from the model published by Bronger for the tellurido salt, the R1 value converged at a rather high value of 0.09. Additionally, some significant residual difference electron density maxima of heights (6−9) $e^- \times 10^{-6}$ pm^{-3} remained at a distance of about 80 pm from the Cs-atom positions and at the center of the cluster anion. A closer inspection of the diffraction images showed that the crystal used for the data collection was composed of two twin domains related by the twin law given in Table 1. Intensities were integrated separately for each component, and the coinciding reflections and integrated data were merged and corrected for absorption using the program *Twinabs*. Because of the very different volumes of the two domains [0.814(2):0.186(2)], only the reflections of the major domain and the coinciding reflections were used for further parameter refinement. The final structure refinement smoothly converged to low R values and left no significant residual electron density in the difference electron density map.

The crystallographic data of both compounds and refined atomic parameters of $Cs_7[Fe_4S_8]$ are summarized in Tables 1 and 2, respectively.[32] Selected interatomic distances are collected in Tables 4 ($Cs_8[Fe_4S_{10}]$) and 5 ($Cs_7[Fe_4S_8]$).

Band-Structure Calculation. DFT calculations of the electronic band structures were performed using the FP-LAPW method (program *Wien2k*[33]) for the two title compounds. The exchange-correlation contribution was described by the generalized gradient approximation (GGA) of Perdew, Burke, and Ernzerhof.[34] Muffin-tin radii were chosen as 111 pm (2.1 au) for all atoms. Cutoff energies used are E_{max}^{pot} = 190 eV (potential) and E_{max}^{wf} = 116 eV (interstitial PW). In the spin-polarized GGA+U calculation, the additional Coulomb potential (Hubbard U parameter) used for the strongly correlated Fe d electrons was 2 eV,[35] and the self-interaction[36,37] double-counting correction method has been applied. AFM spin ordering was applied along the chain piece in $Cs_8[Fe_4S_{10}]$ as well as for two sets of Fe atoms in the Fe_4S_4 cluster of $Cs_7[Fe_4S_8]$. Electron densities were visualized using the programs *XCrysDen*[38] and *DRAWxtl*.[39] A Bader analysis of the electron density distribution was performed to evaluate the charge distribution between the atoms as well as the magnitude and location of the bond critical points (BCPs)[40] using the program *CRITIC2*.[41,42] Further parameters and selected results of the calculations are summarized in Table 3. The total (tDOS) and partial density of states (pDOS) on Fe are depicted in Figure 6.

Table 1. Crystallographic Data, Details of the Data Collection, and Structure Determination for the Sulfido Ferrates $Cs_8[Fe_4S_{10}]$ and $Cs_7[Fe_4S_8]$

compound	$Cs_8[Fe_4S_{10}]$	$Cs_7[Fe_4S_8]$	
temperature [K]	295	100	295
structure type	$Cs_8[Ga_4Se_{10}]$[27]	$Cs_7[Fe_4Te_8]$[28]	
cryst syst	triclinic	monoclinic	
space group, Z	$P\bar{1}$ (No. 2), 1	$C2/c$ (No. 15), 4	
lattice param			
a [pm]	767.83(10)	1891.65(7)	1896.08(9)
b [pm]	885.57(12)	852.92(3)	855.53(4)
c [pm]	1067.7(2)	1668.62(6)	1676.41(8)
α [deg]	79.013(6)		
β [deg]	85.151(6)	117.9501(13)	117.755(2)
γ [deg]	80.185(6)		
volume of the unit cell [$\times 10^6$ pm^3]	701.2(2)	2378.17(15)	2406.5(2)
density (X-ray) [g/cm^3]	3.81	3.94	
diffractometer	Bruker Apex II Quazar (microfocus source, Mo $K\alpha$) rad.		
abs coeff μ(Mo $K\alpha$) [mm^{-1}]	12.99	13.64	
θ range [deg]	1.9−37.0	2.4−33.3	
no. of collected/indep reflns	47520/7027	13298/5567	
R_{int}	0.0417	0.0349	
twin law (real space)		−1 0 −1, 0 −1 0, 0 0 1	
twin ratio		0.814(2):0.186(2)	
corrections	Lorentz, polarization, absorption		
structure refinement	*SHELXL-2013*[29]		
no. of free param	101	88	
GOF on F^2	1.149	1.211	
R values [for refls with $I \geq 2\sigma(I)$]	R1 = 0.0410, wR2 = 0.1193	R1 = 0.0489, wR2 = 0.1200	
R values (all data)	R1 = 0.0458, wR2 = 0.1223	R1 = 0.0507, wR2 = 0.1206	
residual electron density [$e^- \times 10^{-6}$ pm^{-3}]	+5.0/−1.3	+5.1/−3.1	

RESULTS AND DISCUSSION

Syntheses. The two new sulfido ferrates $Cs_8[Fe_4S_{10}]$ and $Cs_7[Fe_4S_8]$ have been obtained in the course of a systematic synthetic study on the phase formation of cesium sulfido ferrates in the narrow composition range at Fe:S ratios between 1:2 and 1:2.5. They could both be obtained in pure phase from stoichiometric samples containing elemental Fe and S with (previously prepared) Cs_2S_2 as the Cs source (and oxidant) at a maximum temperature of 1070 K (cf. Experimental Section). The two cesium sulfido ferrates form xenomorphic crystals with a green metallic luster.

Crystal Structure of $Cs_8[Fe^{III}_4S_{10}]$. $Cs_8[Fe_4S_{10}]$ crystallizes in the $Cs_8[Ga_4Se_{10}]$-type structure[27] and is thus also isotypic to the rubidium ferrate $Rb_8[Fe_4S_{10}]$.[4] These compounds are

dx.doi.org/10.1021/ic502382v | Inorg. Chem. 2015, 54, 1038−1048

Table 2. Atomic Coordinates and Equivalent Isotropic Displacement Parameters [pm^2] in the Crystal Structure of $Cs_7[Fe_4S_8]$

atom	Wyckoff position	x	y	z	U_{equiv}
Cs(1)	4e	0	0.23059(9)	$^1/_4$	115.9(14)
Cs(2)	8f	0.00479(4)	0.24855(8)	0.48611(4)	173.9(13)
Cs(3)	8f	0.23512(3)	0.23914(7)	0.10847(4)	130.7(11)
Cs(4)	8f	0.24079(4)	0.25356(7)	0.36035(4)	146.1(12)
Fe(1)	8f	0.43942(8)	0.11625(15)	0.15933(9)	73(2)
Fe(2)	8f	0.44072(8)	0.34798(15)	0.27923(9)	72(2)
S(1)	8f	0.35769(14)	0.0344(3)	0.54461(16)	114(4)
S(2)	8f	0.13427(13)	0.0013(3)	0.18309(16)	110(4)
S(3)	8f	0.42441(13)	0.0784(2)	0.29058(15)	85(3)
S(4)	8f	0.42174(13)	0.3847(3)	0.13044(15)	91(3)

Table 3. Details and Selected Results of Calculation of the Electronic Structure of $Cs_8[Fe_4S_{10}]$ and $Cs_7[Fe_4S_8]$

		$Cs_8[Fe_4S_{10}]$	$Cs_7[Fe_4S_8]$
crystal data		Tables 1 and 2	
R_{mt} (all atoms)		111.1 pm (2.1 au)	
$R_{mt}K_{max}$		8.0	8.0
k points/BZ		880	864
k points/IBZ		440	234
Monkhorst packing grid		11 × 10 × 8	12 × 12 × 6
DOS plot		Figure 6, top	Figure 6, bottom
	Bond		
ρ_{BCP} [$e^- \times 10^{-6}$ pm^{-3}] (d [pm])	a	0.603 (223.0)	0.610 (222.1)
	b	0.603 (223.0)	0.604 (222.6)
	c	0.602 (222.9)	0.485 (232.8)
	d	0.577 (224.9)	0.480 (233.2)
	e	0.513 (230.9)	0.447 (235.9)
	f	0.499 (232.1)	0.472 (224.9)
	g	0.561 (226.4)	0.466 (226.4)
	h	0.542 (228.1)	0.456 (228.1)
	Atom		
Bader charge (volume [$\times 10^6$ pm^3])	Cs(1)	+0.783 (37.7)	+0.749 (34.3)
	Cs(2)	+0.756 (37.3)	+0.777 (38.3)
	Cs(3)	+0.799 (39.7)	+0.774 (38.0)
	Cs(4)	+0.785 (38.6)	+0.781 (40.6)
	Fe(1)	+1.137 (12.4)	+0.965 (11.9)
	Fe(2)	+1.150 (11.9)	+0.963 (11.9)
	S(1)	−1.136 (35.9)	−1.201 (37.4)
	S(2)	−1.144 (34.6)	−1.214 (36.9)
	S(3)	−1.012 (32.6)	−1.110 (32.7)
	S(4)	−1.070 (36.1)	−1.109 (32.2)
	S(5)	−1.047 (33.5)	

members of the general series $A_{n+4}[Fe_nS_{2n+2}]$ of edge-sharing $[FeS_4]$ tetrahedra between dimers (n = 2) and the common chains (n = ∞). In the crystal structure of $Cs_8[Fe_4S_{10}]$ (i.e., n = 4), four tetrahedra $[FeS_4]$ are connected via opposite (trans) edges to form linear tetramers $[Fe_4S_{10}]^{8-}$. The crystallographically only $\bar{1}$ symmetric anions are depicted in Figure 1 (top left) in an ORTEP representation. Despite their low crystallographic site symmetry, their molecular symmetry differs only slighty from the ideal *mmm* point group symmetry; i.e., the distance pairs a/b (both terminal), c/d, e/f, and g/h (both μ_2 bridging) are very similar (Table 4). The two Fe(2) ions in the "core" of the anion exhibit rather regular Fe−S distances in the range 222.9−228.1 pm. In contrast, the bond lengths in the $[Fe(1)S_4]$ tetrahedra at the anion's periphery are considerably different: The two terminal Fe(1)−S^t distances a and b are both 223.0 pm in length, whereas the bridging Fe(2)−S(3/4) distances are the largest in the ferrate anion ($d^{c/d}_{Fe-S}$ = 230.9/232.1 pm). The averaged Fe−S distances for the two Fe^{III} cations amount to 227.3 pm for Fe(1) and 225.7 pm for Fe(2) and are thus lying between the shorter values in the dimers (e.g., A = Cs: $\bar{d}$ = 227.4 pm) and the chain structures ($\bar{d}$ = 221 pm for A = Rb). The Fe−Fe distances between the central Fe(2) cations of 284.0 pm are slightly shorter than the Fe−Fe contacts toward the terminating Fe(1) cations (288.7 pm). This finding fits the situation in the isotypic rubidium compound[4] and is also consistent with the distances in the related cesium sulfido ferrates(III), where the dimers in $Cs_6[Fe_2S_6]$ (d_{Fe-Fe} = 295.0 pm[9]) exhibit an increased Fe−Fe distance compared to the corresponding chain ferrate $Cs[FeS_2]$ (d_{Fe-Fe} = 269.6/272.5 pm[44]). The angles Fe−S−Fe at the μ_2-S ligands are 77.3−79.0°. The volumes of the $[FeS_4]$ tetrahedra,[39,45] which are a commonly used parameter for the determination of the iron oxidation states in the cluster compounds (see below), amount to 5.962 × 10^6 pm^3 [Fe(1)] and 5.834 × 10^6 pm^3 [Fe(2)].

A perspective view of the unit cell of $Cs_8[Fe_4S_{10}]$ is depicted on the right-hand side of Figure 1. The tetramers $[Fe_4S_{10}]$ are arranged as interrupted chains, running along the $[\bar{1}11]$ direction of the triclinic unit cell. The projection perpendicular to this direction (Figure 1, bottom left) shows the resulting hexagonal rod packing of the (interrupted) chains, which corresponds to the arrangement in all ferrates $A[FeS_2]$ with $[FeS_{4/2}]$ chains (cf. the review in ref 4). Starting from the infinite-chain anions $[FeS_{4/2}]$, every sixth S_2 edge is substituted by two Cs(2) cations and the centers of the two adjacent former tetrahedra are no longer occupied by Fe. The remaining cations Cs(1), Cs(3), and Cs(4), like all A cations in the chain ferrates, separate the anionic rods from each other.

Like in the dimers $[Fe_2S_6]^{6-}$ in $Cs_6[Fe_2S_6]$,[9] the terminal S ligands of the tetramers $[Fe_4S_{10}]^{8-}$ are coordinated by one Fe and six Cs atoms, whereby the S−Cs distances are found in the range 332.7−366.7 pm. The coordinations of the μ_2-sulfido ligands S(3) and S(4) are 2Fe + 6Cs and 2Fe + 7Cs, respectively. The central bridging anion S(5) is surrounded by two Fe and four Cs cations only.

As was already discussed by Deiseroth for the isotypic selenido gallate $Cs_8[Ga_4Se_{10}]$,[27] the coordination number (CN) of the Cs(2) cation, which is disrupting the ferrate chains, is remarkably small (5). Conversely, the remaining Cs cations exhibit larger, more common CNs of 6 + 1, 6 + 3 and 5 + 3,

dx.doi.org/10.1021/ic502382v | Inorg. Chem. 2015, 54, 1038−1048

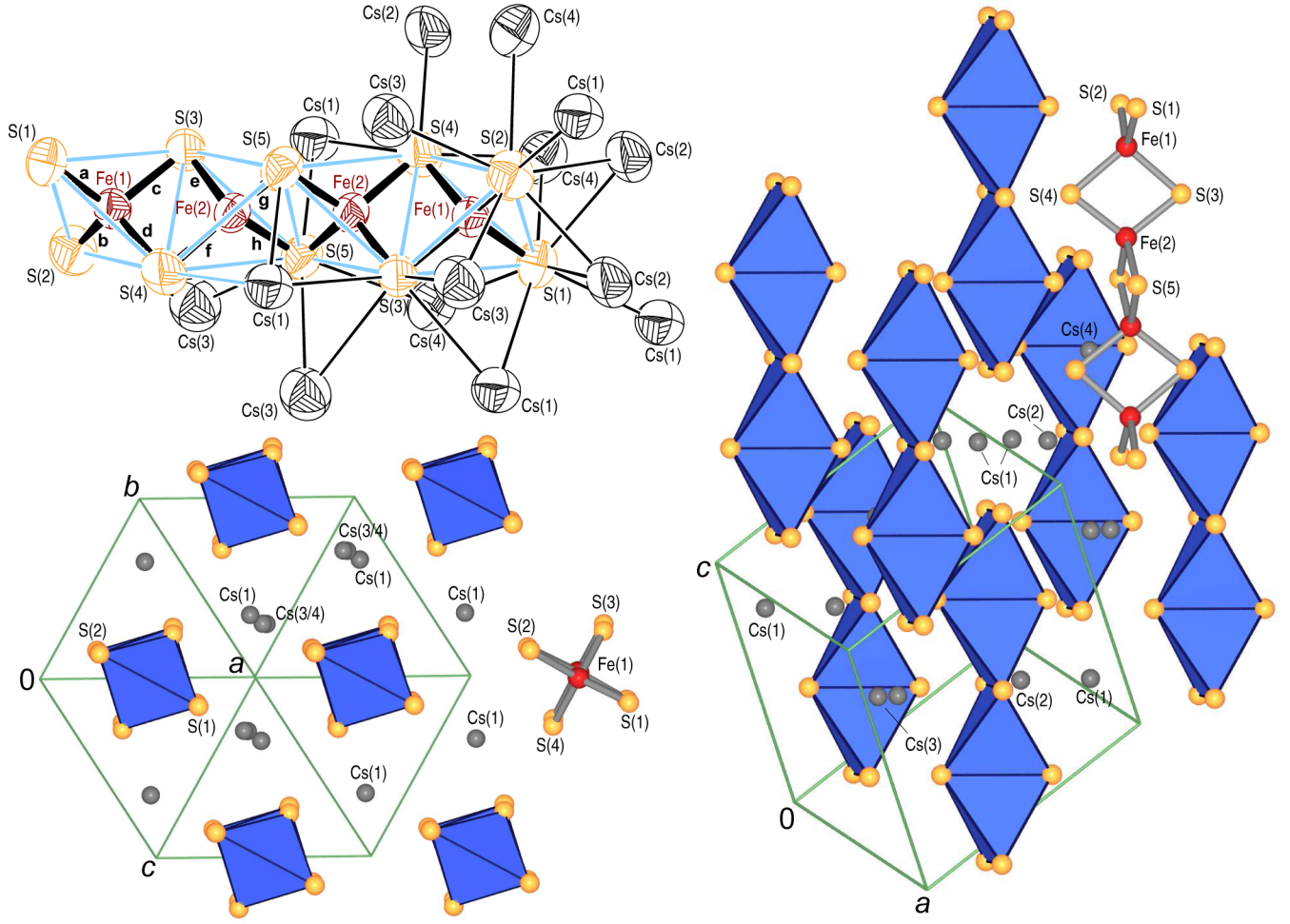

Figure 1. Crystal structure of $Cs_8[Fe_4S_{10}]$. Top left: $[Fe_4S_{10}]$ sulfido ferrate tetramers with the Cs cations surrounding the sulfido ligands in an ORTEP representation (99% probability ellipsoids[43]). Right: Perspective view of the unit cell. Bottom left: Projection onto the $[\bar{1}11]$ plane (gold balls, S; dark gray balls, Cs; blue polyhedra, $[FeS_4]$ tetrahedra[39]). Selected interatomic distances are collected in Table 4.

with a set six/five shorter S−Cs distances below 380 pm and one/three larger contact(s) inbetween 400 and 440 pm (cf. Table 4). Correspondingly, the calculated effective coordination number (ECoN[46,47]) of Cs(2) amounts to 4.989 only, whereas the remaining Cs cations show ECoN values between 5.926 [Cs(3)] and 6.305 [Cs(1)]. The latter values are also similar to those observed for the second title compound (see below).

Crystal Structure of $Cs_7[Fe^{II/III}_4S_8]$. Similar to $Cs_8[Fe_4S_{10}]$, the crystal structure of $Cs_7[Fe_4S_8]$ also contains tetramers of four edge-sharing $[FeS_4]$ tetrahedra. In this mixed-valent ferrate, however, the four tetrahedra are connected to form only slightly distorted tetrahedral $[Fe_4S_8]^{7-}$ anions with a $[Fe_4(\mu_3\text{-}S)_4]^{+}$ cubane core resembling the prominent clusters in the active site of ferredoxins $[Fe_4(\mu_3\text{-}S)_4]^{n+}(S_{cys})_4$ (n = 1, 2), where the positions of the four terminal sulfido ligands are commonly taken by the S atoms of cysteinate.[48] Because of the uncertainty in the exact position of the atoms resulting from the limited resolution of protein crystal diffraction data and the mostly unknown oxidation state, a large series of synthetic analogues of such Fe/S cluster compounds have been extensively studied, where the cysteine ligands are exchanged by halogens X^-, $^-$SH, or $^-$SR.[49,50] Nevertheless, clusters with pure S^{2-} ligands, e.g., simple sulfido ferrate ions of the general formula $[Fe_4S_8]^{n-}$, like those present in the new cesium salt $Cs_7[Fe_4S_8]$, are not yet known. The anion $[Fe_4S_8]^{7-}$ in $Cs_7[Fe_4S_8]$, which exhibits crystallographic point group 2 (C_2) only, is depicted in Figure 2 in an ORTEP representation. On the left-hand side of this figure, the Fe and S atoms are shown exclusively (together with the distance labeling scheme used in Table 5). The right-hand side of Figure 2 shows the full cesium surrounding of the tetramer as well.

According to the nearly $\bar{4}3m$ point group symmetry, each tetrahedrally coordinated Fe(1/2) cation exhibits one short Fe−S^t distance to the terminal μ_1-S ligand S(1/2) ($d^{a,b}_{Fe-S}$ = 222.1(3) and 222.6(2) pm; Table 5) and three likewise very similar bonds toward the μ_3-sulfido ligands S(3) and S(4) (d^{c-h}_{Fe-S} = 232.8−235.9 pm). Because of the averaged oxidation state of Fe in $[Fe_4S_8]^{7-}$ of +2.25 (3 × +II and 1 × +III), the bridging Fe−S bonds are slightly longer than those in the linear tetramer of $Cs_8[Fe_4S_{10}]$ ($\overline{d}^{c-h}_{Fe-S}$ = 227.6 pm). The intracubane-type Fe−S(3,4) distances are somewhat enlarged compared with the distances in the similarly charged $[Fe_4S_4]^{+}$ cluster core of $(Et_4N)_3[Fe_4S_4(SH)_4]\cdot Et_4NCl$[51] (230.9/231.0 pm). As expected, the terminal Fe−S bond lengths of the fully protonated cluster in this compound are with 231.7 pm much larger than the terminal distances a and b in the cesium salt.

The geometry of the $[Fe_4S_4]^{n+}$ cubane-type clusters in natural and biomimetic model compounds has already been extensively studied by Holm et al.[49,50,52] For a set of cluster

dx.doi.org/10.1021/ic502382v | Inorg. Chem. 2015, 54, 1038−1048

Table 4. Selected Interatomic Distances [pm] in the Crystal Structure of $Cs_8[Fe_4S_{10}]$

atoms	distance	bd.[a]	CN	atoms	distance	bd.[a]	CN	atoms	distance	bd.[a]	CN	atoms	distance	bd.[a]	CN
Cs(1)−S(2)	332.7(1)			Cs(2)−S(4)	341.1(1)			Cs(3)−S(2)	335.5(2)			Cs(4)−S(1)	338.2(1)		
Cs(1)−S(5)	349.5(1)			Cs(2)−S(2)	343.9(2)			Cs(3)−S(5)	355.9(1)			Cs(4)−S(5)	342.5(1)		
Cs(1)−S(1)	352.9(1)			Cs(2)−S(2)	344.4(2)			Cs(3)−S(5)	358.5(1)			Cs(4)−S(1)	359.9(1)		
Cs(1)−S(3)	356.0(1)			Cs(2)−S(1)	346.9(1)			Cs(3)−S(2)	366.6(2)			Cs(4)−S(2)	366.7(2)		
Cs(1)−S(1)	361.4(1)			Cs(2)−S(1)	351.6(1)		5	Cs(3)−S(3)	376.6(1)			Cs(4)−S(4)	377.3(2)		
Cs(1)−S(3)	367.4(1)							Cs(3)−S(3)	382.0(1)			Cs(4)−S(3)	403.3(1)		
Cs(1)−S(4)	392.7(2)		6 + 1					Cs(3)−S(3)	429.9(2)			Cs(4)−S(4)	405.6(2)		
								Cs(3)−S(4)	433.1(2)			Cs(4)−S(4)	406.2(2)		5 + 3
								Cs(3)−S(4)	443.6(2)		6 + 3				
Fe(1)−S(1)	223.0(1)	a		Fe(2)−S(3)	222.9(1)	e		S(1)−Fe(1)	223.0(1)	a		S(2)−Fe(1)	223.0(1)	b	
Fe(1)−S(2)	223.0(1)	b		Fe(2)−S(4)	224.9(1)	f		S(1)−Cs(4)	338.2(1)			S(2)−Cs(1)	332.7(1)		
Fe(1)−S(3)	230.9(1)	c		Fe(2)−S(5)	226.4(1)	g		S(1)−Cs(2)	346.9(1)			S(2)−Cs(3)	335.5(2)		
Fe(1)−S(4)	232.1(1)	d	4	Fe(2)−S(5)	228.1(1)	h	4	S(1)−Cs(2)	351.6(1)			S(2)−Cs(2)	343.9(2)		
Fe(1)−Fe(2)	288.7(1)	u		Fe(2)−Fe(2)	284.0(1)	v		S(1)−Cs(1)	352.9(1)			S(2)−Cs(2)	344.4(2)		
				Fe(2)−Fe(1)	288.7(1)	u		S(1)−Cs(4)	359.9(1)			S(2)−Cs(3)	366.6(2)		
								S(1)−Cs(1)	361.4(1)		1 + 6	S(2)−Cs(4)	366.7(2)		1 + 6
S(3)−Fe(2)	222.9(1)	e		S(4)−Fe(2)	224.9(1)	f		S(5)−Fe(2)	226.4(1)	g					
S(3)−Fe(1)	230.9(1)	c		S(4)−Fe(1)	232.1(1)	d		S(5)−Fe(2)	228.1(1)	h					
S(3)−Cs(1)	356.0(1)			S(4)−Cs(2)	341.1(1)			S(5)−Cs(4)	342.5(1)						
S(3)−Cs(1)	367.4(1)			S(4)−Cs(4)	377.3(2)			S(5)−Cs(1)	349.5(1)						
S(3)−Cs(3)	376.6(1)			S(4)−Cs(1)	392.7(2)			S(5)−Cs(3)	355.9(1)						
S(3)−Cs(3)	382.0(1)			S(4)−Cs(4)	405.6(2)			S(5)−Cs(3)	358.5(1)		2 + 4				
S(3)−Cs(4)	403.3(1)			S(4)−Cs(4)	406.2(2)										
S(3)−Cs(3)	429.9(2)		2 + 6	S(4)−Cs(3)	433.1(2)										
				S(4)−Cs(3)	443.6(2)		2 + 7								

[a]Labels for the Fe−S and Fe−Fe bonds; cf. Figure 1).

dx.doi.org/10.1021/ic502382v | Inorg. Chem. 2015, 54, 1038−1048

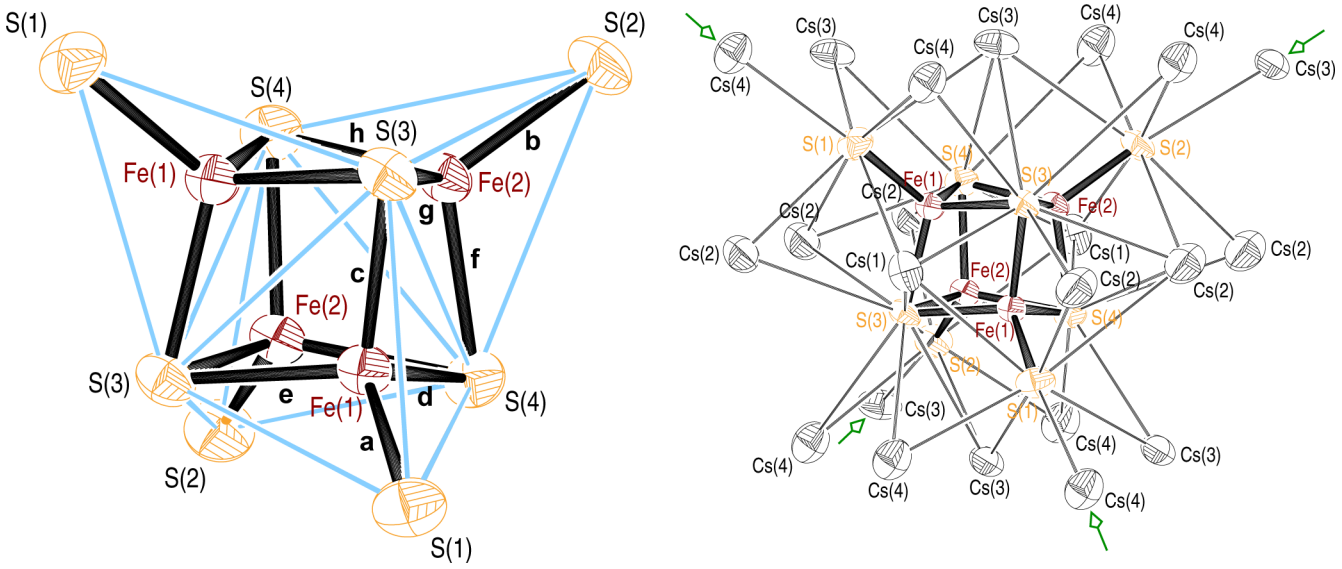

Figure 2. ORTEP view of the cluster $[Fe_4S_8]^{7-}$ in the crystal structure of $Cs_7[Fe_4S_8]$, together with it being surrounded by Cs cations (cf. Table 5 for interatomic distances; 99% ellipsoid probability[43]).

compounds with similar ligands, the volume of the cubane core decreases slightly with increasing iron oxidation state. A strong distortion from the tetrahedral symmetry is only observed for the synthetic all-ferrous example; in ferredoxins (and likewise HiPIP proteins) and also in the title compound $Cs_7[Fe_4S_8]$, the deviations from the tetrahedral symmetry are rather small. Commonly, the volume of the "stella quadrangula" cluster is calculated[52] by summing up the volume of the inner Fe_4 tetrahedron (2.625×10^6 pm^3 in $Cs_7[Fe_4S_8]$) and the four flattened $[Fe_3S]$ tetrahedra (1.930 and 1.925×10^6 pm^3). For $Cs_7[Fe_4S_8]$, this calculation thus results in a cluster volume of 10.34×10^6 pm^3, which is larger than the volumes of all synthetic model compounds, where the cluster volumes, depending on the charge and the types of terminal ligands, amount to $(9.5-10) \times 10^6$ pm^3. Consequently, the Fe−Fe bond lengths in the cesium salt are found above 280 pm (280.4−283.4 pm); in the halogenides and RS^- compounds as well as in the protein-bound clusters, they always lie below this threshold. The reasons for this distinct enlargement of the cluster core in the title compound are certainly the Coulomb repulsion between the comparatively more negatively charged terminal and the μ_3-S atoms, on the one hand, and the Coulomb attraction between the overall most negatively charged ferrate anion and the surrounding Cs^+ cations, on the other hand.

The μ_3-bridging S(3) and S(4) cluster S atoms are, in addition to the three Fe ions, coordinated by six Cs cations at distances between 347.9 and 445.1 pm, resulting in an overall CN of 3 + 6 (Table 5). The six Cs cations are arranged in a flattended trigonal-prismatic shape around the pseudo-3-fold axis of the cluster. The terminal S(1) and S(2) sulfido ligands exhibit a 1 + 7 coordination surrounded by Fe and Cs cations with somewhat shorter S−Cs distances in the range 338.6−414.6 pm. According to Fe:3Cs:3Cs:1Cs, six of the seven Cs cations likewise form a flattened trigonal antiprism around the cluster's pseudo-3-fold axis. The Cs(3/4) "caps" of the prisms form four (marked by arrows in Figure 2) of the eight corners of a large cube of 26 Cs cations, which enclose each $[Fe_4S_8]^{7-}$ ferrate cluster (cf. Figure 3). These large Cs cubes are a useful structure element for the description of the overall crystal structure of $Cs_7[Fe_4S_8]$ (see below). The 26 Cs cations surrounding the sulfido ferrate anions are located at the 8 corners, 6 faces, and 12 edges of the large cube. These cluster-centered cubes are densely packed, whereby they are identically stacked along the *b* axis. Along the *a* axis and the perpendicular direction (2a + c), they are arranged in shifted positions (cf. colored balls, i.e., cluster centers, in Figure 5). This dense stacking of cubes finally results in the overall seven Cs countercations per cube/cluster as follows: Each of the two Cs(1) faces participates in two cubes (2/2 = 1). The six Cs(2) atoms in the cluster-containing layers form the edges and faces of the cubes and contribute to three cubes each (6/3 = 2). The eight Cs(3) atoms (at two faces, two edges, and four corners) participate in four cubes (8/4 = 2), and the 10 Cs(4) cations located at six edges and four corners are assigned to five cubes (10/5 = 2).

According to this arrangement of cluster-centered cubes, a crystallographic group−subgroup relationship can be established between the simple cubic packing (α-Po-type structure) and the packing of cluster anions and Cs cations (in a 1:7 ratio) in the structure of $Cs_7[Fe_4S_8]$. The belonging group−subgroup tree by Bärnighausen[53−56] is depicted in a simplified representation in Figure 4. The symmetry reduction of an overall order of 192 is divided into two different sets: In the first three steps (overall index 12), the site symmetry of the Po atom position is reduced solely by translationengleiche symmetry reductions ($Pm\bar{3}m \xrightarrow{t3} P4/mmm \xrightarrow{t2} Pmmm \xrightarrow{t2} P2/m$; i.e., the unit cell remains unchanged; Figure 4, top left). The atom position can be shifted in one of the last two steps from 0, 0, 0 to 0, $^1/_2$, 0. In the second series of symmetry reductions with an overall index 16, the monoclinic unit cell is successively enlarged by applying four klassengleiche (k) or isomorphic (i) symmetry reductions ($P2/m \xrightarrow[a=2a-c]{i2} P2/m \xrightarrow[c=2c]{i2} P2/m \xrightarrow[a=2a,b=2b]{k2} C2/m \xrightarrow[c=2c]{k2} C2/c$). (The first of these steps is evidentally the origin of the observed twinning; cf. the Experimental Section.) These four symmetry reductions involve an enlargement of the unit cell by a factor of 32 (16 × 2, due to the *C* centering of the final unit cell) by applying the overall matrix

dx.doi.org/10.1021/ic502382v | Inorg. Chem. 2015, 54, 1038−1048

Table 5. Selected Interatomic Distances [pm] in the Crystal Structure of $Cs_7[Fe_4S_8]$

atoms	distance	bd.[a]	CN	atoms	distance	bd.[a]	CN	atoms	distance	bd.[a]	CN	atoms	distance	bd.[a]	CN
Cs(1)−S(4) (2×)	347.9(2)			Cs(2)−S(1)	342.2(2)			Cs(3)−S(2)	339.6(2)			Cs(4)−S(1)	338.6(2)		
Cs(1)−S(3) (2×)	349.5(2)			Cs(2)−S(2)	351.8(2)			Cs(3)−S(1)	342.7(2)			Cs(4)−S(2)	344.2(2)		
Cs(1)−S(2) (2×)	376.6(2)			Cs(2)−S(4)	362.0(2)			Cs(3)−S(4)	359.5(2)			Cs(4)−S(1)	346.8(2)		
Cs(1)−S(1) (2×)	379.0(2)		8	Cs(2)−S(3)	363.0(2)			Cs(3)−S(3)	370.6(2)			Cs(4)−S(2)	349.0(2)		
				Cs(2)−S(2)	371.5(2)			Cs(3)−S(1)	377.8(2)			Cs(4)−S(3)	405.1(2)		
				Cs(2)−S(3)	402.8(2)			Cs(3)−S(4)	383.7(2)			Cs(4)−S(3)	440.9(2)		
				Cs(2)−S(1)	414.6(2)			Cs(3)−S(2)	389.2(2)		7	Cs(4)−S(4)	445.1(2)		4 + 3
				Cs(2)−S(4)	422.8(2)		5 + 3								
Fe(1)−S(1)	222.1(3)	a		Fe(2)−S(2)	222.6(2)	b									
Fe(1)−S(3)	232.8(3)	c		Fe(2)−S(4)	233.7(3)	f									
Fe(1)−S(4)	233.2(2)	d		Fe(2)−S(3)	233.9(2)	g									
Fe(1)−S(3)	235.9(2)	e	4	Fe(2)−S(4)	235.7(3)	h	4								
Fe(1)−Fe(2)	280.4(2)			Fe(2)−Fe(1)	280.4(2)										
Fe(1)−Fe(1)	281.2(3)			Fe(2)−Fe(1)	281.4(2)										
Fe(1)−Fe(2)	281.4(2)			Fe(2)−Fe(2)	283.4(2)										
S(1)−Fe(1)	222.1(3)	a		S(2)−Fe(2)	222.6(2)	b		S(3)−Fe(1)	232.8(3)	c		S(4)−Fe(1)	233.2(2)	d	
S(1)−Cs(4)	338.6(2)			S(2)−Cs(3)	339.6(2)			S(3)−Fe(2)	233.9(2)	g		S(4)−Fe(2)	233.7(3)	f	
S(1)−Cs(2)	342.2(2)			S(2)−Cs(4)	344.2(2)			S(3)−Fe(1)	235.9(2)	h		S(4)−Fe(2)	235.7(3)	h	
S(1)−Cs(3)	342.7(2)			S(2)−Cs(4)	349.0(2)			S(3)−Cs(1)	349.5(2)			S(4)−Cs(1)	347.9(2)		
S(1)−Cs(4)	346.8(2)			S(2)−Cs(2)	351.8(2)			S(3)−Cs(2)	363.0(2)			S(4)−Cs(3)	359.5(2)		
S(1)−Cs(3)	377.8(2)			S(2)−Cs(2)	371.5(2)			S(3)−Cs(3)	370.6(2)			S(4)−Cs(2)	362.0(2)		
S(1)−Cs(1)	379.0(2)			S(2)−Cs(1)	376.6(2)			S(3)−Cs(2)	402.8(2)			S(4)−Cs(3)	383.7(2)		
S(1)−Cs(2)	414.6(2)		1 + 7	S(2)−Cs(3)	389.2(2)		1 + 7	S(3)−Cs(4)	405.1(2)			S(4)−Cs(2)	422.8(2)		
								S(3)−Cs(4)	440.9(2)		3 + 6	S(4)−Cs(4)	445.1(2)		3 + 6

[a]Labels for the Fe−S and Fe−Fe bonds; cf. Figure 2.

dx.doi.org/10.1021/ic502382v | Inorg. Chem. 2015, 54, 1038−1048

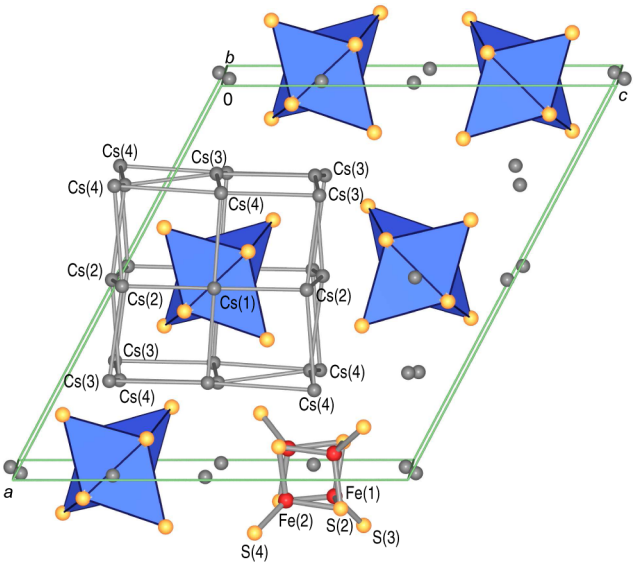

Figure 3. Arrangement and Cs surrounding the sulfido ferrate clusters in the crystal structure of $Cs_7[Fe_4S_8]$ (gold/light gray spheres, S/Cs; blue polyhedra, $[FeS_4]$ tetrahedra; red spheres, Fe[39]).

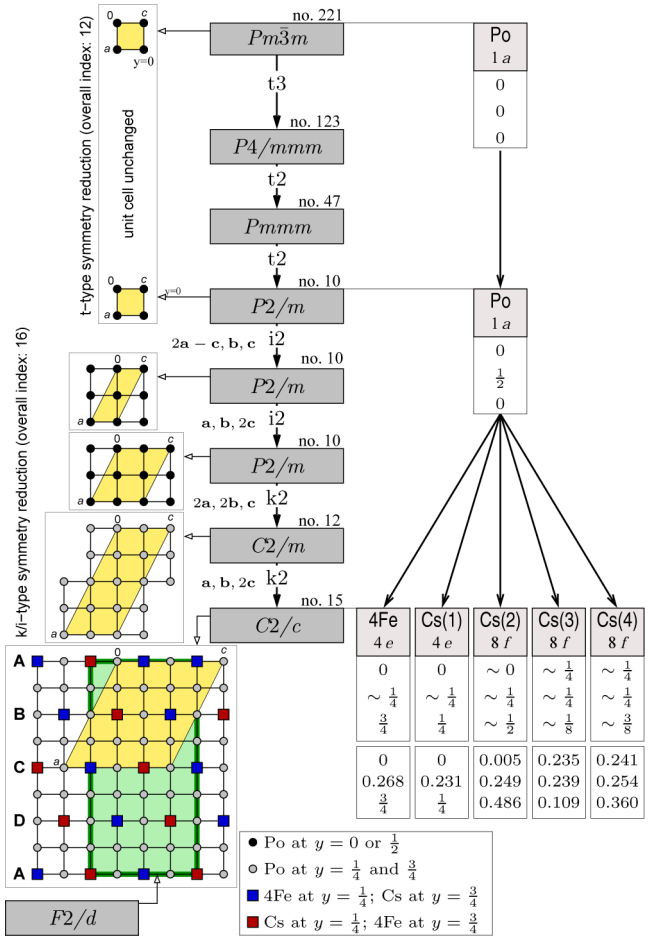

Figure 4. Simplified Bärnighausen group−subgroup tree relating the simple cubic aristotype (α-Po-type structure) with the packing of Cs cations and cluster anions in the structures of $Cs_7[Fe_4S_8]$ (see the text for further details).

4 0 −2/0 2 0/0 0 4, i.e., **a** = 4**a** − 2**c**, **b** = 2**b**, and **c** = 4**c** (see yellow-shaded unit cells in Figure 4). The ideal atomic coordinates calculated from the atom position 0, 0, 0 upon application of this symmetry reduction are shown on the right-hand side of Figure 4 for selected steps only. The coordinates obtained for the final monoclinic *C*2/*c* model are indeed very close to the positions of the four Cs cations and the center of gravity of the tetrameric sulfido ferrate cluster anion (cf. the table in Figure 4). The metric relations belonging to the simple cubic cell with the lattice parameter a', $c = 4a'$, $b = 2a'$, and $a = \sqrt{20}a'$, which were already noticed by Bronger for the isotypic iron telluride,[28,31] also lead to very similar values for a' of 417.16, 426.46, and 422.99 pm, respectively. The symmetry of the stacked cluster-centered cubes in the structure of $Cs_7[Fe_4S_8]$ is easier to identify when using the nonstandard setting *F*2/*d* of the space group *C*2/*c*. The belonging unit cell is indicated by a light-green shading in Figure 4. This cell is recognizably derived by a simple enlargement of the unit cell axes of the pseudocubic α-Po type according to **a** = 8**a**, **b** = 2**b**, and **c** = 4**c**.

The final resulting packing of Cs cations (light gray) and cluster anions (Fe_4 centers marked by colored balls) is additionally shown in a perspective view at the top of Figure 5. Along the long pseudoorthorhombic *a* axis, square-planar pure Cs layers [composed of four Cs(3)/Cs(4) atoms per

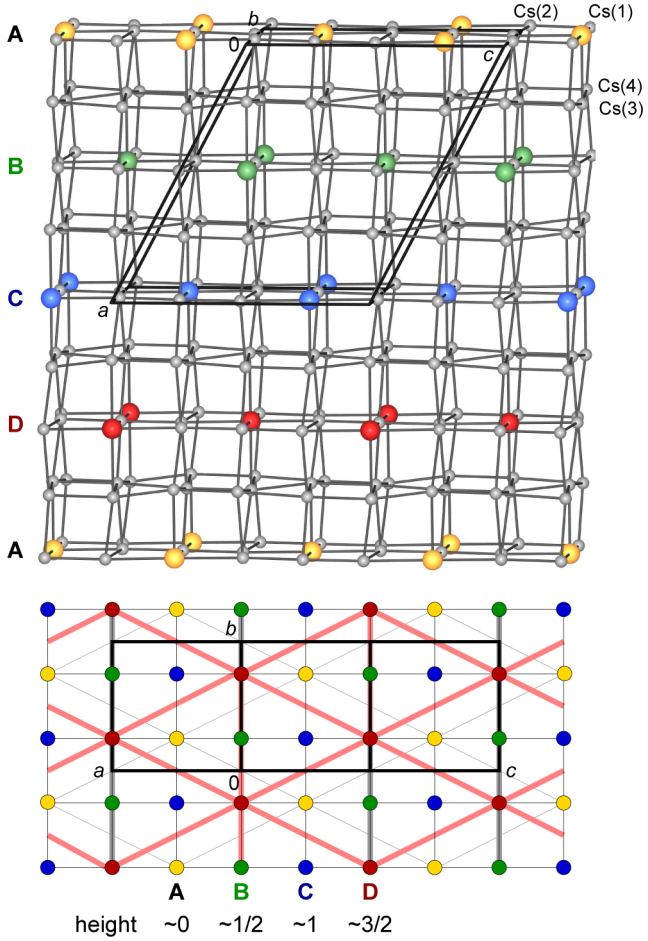

Figure 5. Top: Packing of Cs^+ (light-gray spheres) and Fe_4S_4 clusters (centers shown as colored spheres) in the crystal structure of $Cs_7[Fe_4S_8]$ (cf. Figure 4 for the symmetry relationship belonging between the cubic primitive arrangement of the α-Po-type structure and the Cs/cluster packing[39]); Bottom: Stacking of the layers perpendicular to the *bc* plane.

dx.doi.org/10.1021/ic502382v | Inorg. Chem. 2015, 54, 1038−1048

formula unit] alternate with mixed Cs(1)/Cs(2)/Fe_4 layers labeled as A–D. In these layers, the cluster substitutes a quarter of the Cs cations of the square net, resulting in a Cs:Fe_4 ratio of 3:1 and a pseudohexagonal ordering of the [Fe_4S_4] groups. Along the *a* axis, these "colored" mixed layers are stacked in an A–B–C–D sequence, whereby neighboring layers are shifted against each other along the *c* axis by $z = {}^1/_4$ (Figure 5, bottom).

The Cs cations Cs(1) and Cs(2) contributing to the mixed A–D layers are surrounded by eight S atoms, with Cs–S distances of 342–423 pm (Table 5). The Cs cations of the pure Cs layers are coordinated by seven [Cs(3)] and a 4 + 3 [Cs(4)] S atom only. The connected Cs–S distances are similar (339–445 pm) and also agree well with the atomic distances in $Cs_8[Fe_4S_{10}]$ and the sum of Shannon's radii[57] of Cs^+ and S^{2-} of 358 pm.

Electronic Structures and Chemical Bonding. The electronic band structures of the two title compounds $Cs_8[Fe_4S_{10}]$ and $Cs_7[Fe_4S_8]$ were calculated for antiferromagnetically ordered models (see below) using FP-LAPW DFT methods (GGA + *U*) including spin polarization and a suitable *U* parameter of 2 eV.[35] Computational details can be found in the Experimental Section and are additionally summarized in Table 3. For both compounds, the calculated electron density maps exhibit pronounced BCPs of heights between 0.45 and 0.61 $e^- \times 10^{-6}$ pm^{-3} at the Fe–S contacts with distances between 235.9 and 222.1 pm. As expected, these bond densities nicely correlate with the bond lengths. The Bader charges (and volumes) also meet all expectations: The Fe^{III} ions in $Cs_8[Fe_4S_{10}]$ are slightly more positive (+1.135) compared to the formally 2.25+ charged ions in $Cs_7[Fe_4S_8]$ (0.96+; Table 3).

For the iron(III) ferrate $Cs_8[Fe_4S_{10}]$, an AFM ordering of the Fe spins in the chain segment (↑↓↑↓) has been set up in space group *P*1. Even though not yet experimentally proven, this spin ordering is most probable because of the likewise AFM spin orientation in the dimers $A_6[Fe_2S_6]$[58–60] and the chain ferrates $A[FeS_2]$,[11,61,62] respectively. The calculated tDOS (gray-shaded) and pDOS (red/blue lines) for Fe are depicted in the top part of Figure 6. $Cs_8[Fe_4S_{10}]$ contains 80 valence electrons per formula unit (ve/fu), excluding the S s states [8(8Cs) + 32(4Fe) + 40(10S)]. Overall, 10 × 6 = 60 ve/fu form the S^{2-} p bands, which are located in the energy range between −4 eV and the Fermi level E_F. As expected for an antiferromagnetically ordered high-spin configuration of trivalent Fe, the remaining 4 × 5 = 20 ve/fu are found in both spin states between −5.4 and −4.3 eV. The conduction band is composed of the inverted spin states of Fe and is located inside the large gap between the populated S p bands and the empty Cs states at +3 eV. The resulting band gap of 1 eV is thus associated with a L → M-CT (CT insulator of class 2B) and fits the observed greenish luster of the crystals of $Cs_8[Fe_4S_{10}]$. Starting from an ideal tetrahedron with a small two-under-three splitting of the d orbitals, the addition of further Fe cations along the chain direction causes an increased splitting of the d states connected with an energy lowering of *z*-contributing d orbitals.[11] This splitting is less pronounced for the terminal Fe(1) ions than for the Fe(2) ions inside the chains pieces, which are surrounded by two Fe ions of the neighboring tetrahedra. Consistently, the d states of the central Fe(2) ions in $Cs_8[Fe_4S_{10}]$ at −5.4 eV are the lowest-energy Fe d states.

The band-structure calculation of the new mixed-valent cluster ferrate $Cs_7[Fe_4S_8]$ was performed for the most simple

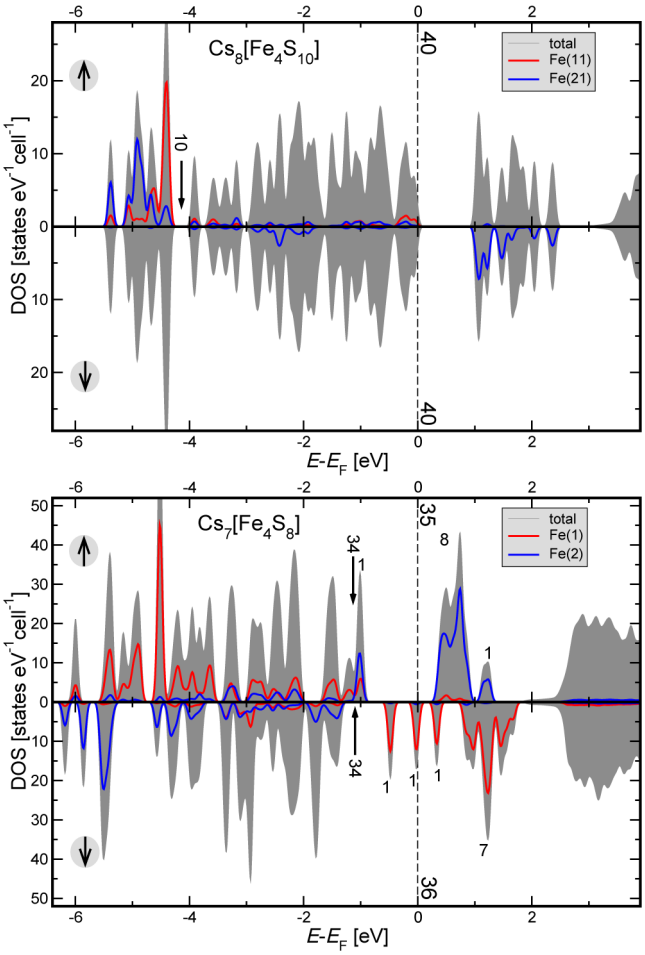

Figure 6. Calculated tDOS (gray) together with pDOS of Fe (red/blue lines) of the title compounds $Cs_8[Fe_4S_{10}]$ (top) and $Cs_7[Fe_4S_8]$ (bottom) in the range between −6.3 and 3.8 eV relative to E_F.

AFM model, where the Fe(1) and Fe(2) atoms of each pair are of similar spin, but the two pairs exhibit opposite spins among each other. This type of AFM ordering is observed for all protein-bound and synthetic $[Fe_4S_4]^{n+}$ clusters.[63] Because of the nearly tetrahedral symmetry of the cluster in $Cs_7[Fe_4S_8]$, alternative models for the AFM spin ordering, e.g., with Fe(1)/Fe(2) pairs of parallel spin, will not fundamentally change the results of the calculation. The number of valence electrons in $Cs_7[Fe_4S_8]$ amounts to 71 per formula unit, again excluding the low-lying s states of S. The 34 bands of lowest energy (34 ve/fu/spin; overall 68 ve; see the arrows in Figure 6) are formed by the majority spin states of Fe^{III} (4 × 5 = 20) and the sulfide p electrons (6 × 8 = 48 ve/fu). In contrast to the more ionic ferrate(III) discussed above, the pronounced mixing of these two orbital types indicates the increased covalency of the Fe–S bonding. The three extra valence electrons of the Fe^{II} d^6 ions of the cluster occupy three different states: At an energy of −1 eV, one $^{\uparrow}$d state of Fe(2) per cluster is occupied. This spin is compensated for by the $^{\downarrow}$d Fe(1) occupied states found at −0.5 eV. The third electron also takes $^{\downarrow}$d Fe(1) orbitals, leading to an overall spin for the cluster of ${}^1/_2$, which is indeed found for all native and synthetic $[Fe_4S_4]^+$ clusters.[63] The exact energy and dispersion of these three bands slightly below E_F, which determines the chemical, physical, and spectroscopic properties of the cluster compound, are highly dependent not only on the AFM model used but also on further parameters of the

dx.doi.org/10.1021/ic502382v | Inorg. Chem. 2015, 54, 1038–1048

theoretical approach. Thus, the first band-structure calculation of an $[Fe_4S_4]$ cluster in the solid state reported herein should not yet be considered conclusive, and further computational as well as spectrocopic (Mössbauer) and magnetic investigations are underway. Irrespective of the exact position of the $^{\downarrow,\uparrow}$Fe(1/2) band energy the optical properties of the compound are determined by electron-transfer processes between the d states of different Fe cations in the cluster.

Summary and Outlook. The two cesium sulfido ferrates $Cs_8[Fe_4S_{10}]$ and $Cs_7[Fe_4S_8]$ were synthesized in pure phase from Fe, S, and Cs_2S_2. They were structurally characterized by means of single-crystal diffraction data. $Cs_8[Fe_4S_{10}]$ is isotypic with the belonging rubidium tetraferrate and exhibits linear tetrameric anions of edge-sharing $[FeS_4]$ tetrahedra. In the structure of the mixed-valent ferrate $Cs_7[Fe_4S_8]$, these tetrahedra are likewise connected via edges to form $[Fe_4S_8]^{7-}$ clusters with a cubane-type $[Fe_4S_4]^{+}$ core. The nearly tetrahedral anions are enclosed by a cube of 26 Cs^+ cations, and the overall crystal structure can be described by the packing of these cubes. Band-structure calculations of antiferromagnetically ordered models show that the pure ferrate(III) exhibits a small band gap associated with L → M-CT. The mixed-valent cluster compound $Cs_7[Fe_4S_8]$ contains the famous puzzling intermediate-valent $[Fe^{II/III}]$, complex-spin system of four antiferromagnetically coupled Fe ions extensively used by nature. For the first time, the purely inorganic solid compound $Cs_7[Fe_4S_8]$ with its very precise structural data (and the known cluster charge) allowed calculation of the electronic structure of this very important structural motif at a current level of FP-LAPW DFT band-structure theory, i.e., using periodic boundary conditions. We are currently pursuing different avenues to further characterize the compounds both computationally (applying different AFM models and levels of theory) and by Mössbauer spectroscopy; unfortunately, the latter is proving to be unexpectedly difficult. Magnetic measurements are also the work of ongoing research.

■ ASSOCIATED CONTENT

Supporting Information

X-ray crystallographic data in CIF format for $Cs_8Fe_4S_{10}$ and $Cs_7Fe_4S_8$. This material is available free of charge via the Internet at http://pubs.acs.org.

■ AUTHOR INFORMATION

Corresponding Author

*E-mail: caroline@ruby.chemie.uni-freiburg.de. Phone: 0049 (0)761 2036143. Fax: 0049 (0)761 2036012.

Notes

The authors declare no competing financial interest.

■ ACKNOWLEDGMENTS

The authors thank the Deutsche Forschungsgemeinschaft for financial support.

■ REFERENCES

(1) Bronger, W.; Müller, P. *J. Alloys Compd.* **1997**, *246*, 27−36.
(2) Bronger, W. *Angew. Chem., Int. Ed. Engl.* **1981**, *20*, 52−62.
(3) Harrison, M. R.; Francesconi, M. G. *Coord. Chem. Rev.* **2011**, *255*, 451−458.
(4) Schwarz, M.; Haas, M.; Röhr, C. *Z. Anorg. Allg. Chem.* **2013**, *639*, 360−374.
(5) Bronger, W.; Balk-Hardtdegen, H.; Ruschewitz, U. *Z. Anorg. Allg. Chem.* **1992**, *616*, 14−18.
(6) Klepp, K. O.; Bronger, W. *Z. Anorg. Allg. Chem.* **1986**, *532*, 23−30.
(7) Bronger, W.; Ruschewitz, U. *J. Alloys Compd.* **1993**, *197*, 83−86.
(8) Müller, P.; Bronger, W. *Z. Naturforsch.* **1979**, *34b*, 1264−1266.
(9) Bronger, W.; Ruschewitz, U.; Müller, P. *J. Alloys Compd.* **1992**, *187*, 95−103.
(10) Boller, H.; Blaha, H. *Monatsh. Chem.* **1983**, *114*, 145−154.
(11) Bronger, W.; Kyas, A.; Müller, P. *J. Solid State Chem.* **1987**, *70*, 262−270.
(12) Pant, A. K.; Stevens, E. D. *Phys. Rev. B* **1988**, *37*, 1109−1120.
(13) Smyk, A. A.; Sablina, K. A.; Kokov, I. T. *Kristallografiya* **1989**, *34*, 757−758.
(14) Klepp, K.; Boller, H. *Monatsh. Chem.* **1981**, *112*, 83−89.
(15) Bronger, W.; Ruschewitz, U.; Müller, P. *J. Alloys Compd.* **1995**, *218*, 22−27.
(16) Amthauer, G.; Bente, K. *Naturwissensch.* **1983**, *70*, 146−147.
(17) Boller, H. *Acta Crystallogr.* **2004**, *A60*, s47.
(18) Mitchell, R. H.; Ross, K. C.; Potter, E. G. *J. Solid State Chem.* **2004**, *177*, 1867−1872.
(19) Schwarz, M.; Röhr, C. *Z. Kristallogr. Suppl.* **2014**, *34*, 149.
(20) Lei, H.; Abeykoon, M.; Bozin, E. S.; Wang, K.; Warren, J. B.; Petrovic, C. *Phys. Rev. Lett.* **2011**, *107*, 137002.
(21) Lei, H.; Abeykoon, M.; Bozin, E. S.; Petrovic, C. *Phys. Rev. B* **2011**, *83*, 180503.
(22) Lazarević, N.; Lei, H.; Petrovic, C.; Popović, Z. V. *Phys. Rev. B* **2011**, *84*, 214305.
(23) Schwarz, M.; Röhr, C. *Z. Anorg. Allg. Chem.* **2014**, *640*, 2792−2800.
(24) Evans, H. T.; Clark, J. R. *Am. Mineral.* **1981**, *66*, 376−384.
(25) Brauer, G. *Handbuch der präparativen anorganischen Chemie*; Enke Verlag: Stuttgart, Germany, 1981.
(26) Yvon, K.; Jeitschko, W.; Parthé, E. *Program Lazy-Pulverix*; University of Geneva: Geneva, Switzerland, 1976.
(27) Deiseroth, H. J. *Z. Kristallogr.* **1984**, *166*, 283−295.
(28) Bronger, W.; Kimpel, M.; Schmitz, D. *Acta Crystallogr.* **1983**, *B39*, 235−238.
(29) Sheldrick, G. M. *Acta Crystallogr.* **2008**, *A64*, 112−122.
(30) Bronger, W.; Kimpel, M.; Schmitz, D. *Angew. Chem., Int. Ed.* **1982**, *21*, 544.
(31) Bronger, W.; Bomba, C.; Fleischhauer, J.; Rusbüldt, C. *J. Less-Common Met.* **1990**, *167*, 161−167.
(32) Further details on the crystal structure investigations are available from the Fachinformationszentrum Karlsruhe, Gesellschaft für wissenschaftlich-technische Information mbH, D-76344 Eggenstein-Leopoldshafen 2, Karlsrhue, Germany, on quoting the depository numbers CSD-428509 ($Cs_8Fe_4S_{10}$) and CSD-428508 ($Cs_7Fe_4S_8$), the names of the authors, and citation of the paper (E-mail: crysdata@fiz−karlsruhe.de).
(33) Blaha, P.; Schwarz, K.; Madsen, G. K. H.; Kvasnicka, D.; Luitz, J. *Wien2k, An Augmented Plane Wave and Local Orbital Program for Calculating Crystal Properties*; TU Wien: Wien, Austria, 2006; ISBN3-9501031-1-2.
(34) Perdew, J. P.; Burke, S.; Ernzerhof, M. *Phys. Rev. Lett.* **1996**, *77*, 3865−3868.
(35) Rohrbach, A.; Hafner, J.; Kresse, G. *J. Phys.: Condens. Matter* **2003**, *15*, 979−996.
(36) Anisimov, V. I.; Solovyev, I. V.; Korotin, M. A.; Czyzyk, M. T.; Sawatzky, G. A. *Phys. Rev. B* **1993**, *48*, 16929.
(37) Lichtenstein, A. I.; Anisimov, V. I.; Zaanen, J. *Phys. Rev. B* **1995**, *52*, R5467.
(38) Kokalj, A. *J. Mol. Graphics Modell.* **1999**, *17*, 176−178.
(39) Finger, L. W.; Kroeker, M.; Toby, B. H. *J. Appl. Crystallogr.* **2007**, *40*, 188−192.
(40) Bader, R. W. F. *Atoms in Molecules. A Quantum Theory*; International Series of Monographs on Chemistry; Clarendon Press: Oxford, U.K., 1994.
(41) Otero-de-la-Roza, A.; Blanco, M. A.; Martá, A.; Pendás, A. M.; Luaña, V. *Comput. Phys. Commun.* **2009**, *180*, 157−166.

(42) Otero-de-la Roza, A.; Luaña, V. *J. Comput. Chem.* **2010**, *32*, 291−305.
(43) Burnett, M. N.; Johnson, C. K. *Program Ortep-III. ORNL-6895*; Oak Ridge National Laboratory: Oak Ridge, TN, 1996.
(44) Bronger, W.; Müller, P. *J. Less-Common Met.* **1980**, *70*, 253−262.
(45) Finger, L. W.; Ohashi, Y. *Volcal: Program to Calculate Polyhedral Volumes and Distortion Parameters with Errors*, 1979.
(46) Hoppe, R. *Z. Kristallogr.* **1979**, *150*, 23−52.
(47) Nespolo, M. *Chardi-IT*, version 2007; Nancy-Université: Lorraine, France, 2006.
(48) Beinert, H.; Holm, R. H.; Münck, E. *Science* **1997**, *277*, 653−659.
(49) Lee, S. C.; Lo, W.; Holm, R. H. *Chem. Rev.* **2014**, *114*, 3579−3600.
(50) Rao, P. V.; Holm, R. H. *Chem. Rev.* **2004**, *104*, 527−559.
(51) Segal, B. M.; Hoveyda, H. R.; Holm, R. H. *Inorg. Chem.* **1998**, *37*, 3440−3443.
(52) Tan, L. L.; Holm, R. H.; Lee, S. C. *Polyhedron* **2013**, *58*, 206−217.
(53) Aroyo, M. I.; Perez-Mato, J. M.; Capillas, C.; Kroumova, E.; Ivantchev, S.; Madariaga, G.; Kirov, A.; Wondratschek, H. *Z. Kristallogr.* **2006**, *221*, 15−27.
(54) Aroyo, M. I.; Kirov, A.; Capillas, C.; Perez-Mato, J. M.; Wondratschek, H. *Acta Crystallogr.* **2006**, *A62*, 115−128.
(55) Bärnighausen, H. *MATCH, Commun. Math. Comput. Chem.* **1980**, *9*, 139−175.
(56) Müller, U. *Z. Anorg. Allg. Chem.* **2004**, *630*, 1519−1537.
(57) Shannon, R. D. *Acta Crystallogr.* **1976**, *A32*, 751−767.
(58) Welz, D.; Bennington, S. M.; Müller, P. *Physica B* **1995**, *213&214*, 339−341.
(59) Bronger, W.; Müller, P.; Welz, D. *Physica B* **2000**, *276−278*, 710−711.
(60) Mödl, M.; Povill, A.; Rubio, J.; Illas, F. *J. Phys. Chem. A* **1997**, *101*, 1526−1531.
(61) Bronger, W. *Z. Anorg. Allg. Chem.* **1968**, *359*, 225−233.
(62) Nishi, M.; Ito, Y. *Solid State Commun.* **1979**, *30*, 571−574.
(63) Noodlman, L.; Peng, C. Y.; Case, D. A.; Mouesca, J.-M. *Coord. Chem. Rev.* **1995**, *144*, 199−244.